

Investigating the effect of cosmic opacity on standard candles

J. Hu¹, H. Yu¹ and F. Y. Wang^{1,2*}

¹ *School of Astronomy and Space Science, Nanjing University, Nanjing 210093, China*

² *Key Laboratory of Modern Astronomy and Astrophysics (Nanjing University), Ministry of Education, Nanjing 210093, China*

fayinwang@nju.edu.cn

ABSTRACT

Standard candles can probe the evolution of dark energy in a large redshift range. But the cosmic opacity can degrade the quality of standard candles. In this paper, we use the latest observations, including type Ia supernovae (SNe Ia) from JLA sample and Hubble parameters, to probe the opacity of the universe. In order to avoid the cosmological dependence of SNe Ia luminosity distances, a joint fitting of the SNe Ia light-curve parameters, cosmological parameters and opacity is used. In order to explore the cosmic opacity at high redshifts, the latest gamma-ray bursts (GRBs) are used. At high redshifts, cosmic reionization process is considered. We find that the sample supports an almost transparent universe for flat Λ CDM and XCDM models. Meanwhile, free electrons deplete photons from standard candles through the (inverse) Compton scattering, known as an important component of opacity. This Compton dimming may play an important role in future supernova surveys. From analysis, we find that about a few percent cosmic opacity is caused by Compton dimming in the two models, which can be correctable.

Subject headings: cosmology: theory - distance scale

1. Introduction

In 1998, the accelerating expansion of the universe was discovered by measuring the relation between redshift and distance of SNe Ia (Riess et al. 1998; Perlmutter et al. 1999). The physical origin of accelerating is still debated. The term “dark energy” is put forward to explain the accelerating universe. Meanwhile, the modification of equations governing gravity can also explain the acceleration of the universe (i.e., Capozziello 2002). Besides SNe Ia, other observations, such as cosmic microwave background (CMB) (i.e., Spergel et al. 2003),

baryonic acoustic oscillations (BAO) (i.e., Eisenstein et al. 2005), Hubble parameters (i.e., Jimenez et al. 2003), and gamma-ray bursts (GRBs) (i.e., Wang et al. 2015), can probe the nature of accelerating expansion.

SNe Ia are ideal standard candles to probe dark energy. But several effects can degrade their quality, such as the dust in light path (Avgoustidis et al. 2009), the possible intrinsic evolution in SN luminosity, gravitational lensing magnification (Holz 1998), peculiar velocity (Hui & Greene 2006), and so on. These processes will degrade the standard candle usefulness of SNe Ia. Besides the above effects, Compton dimming due to free electrons deplete photons from standard candles by the (inverse) Compton scattering can cause systematic error for cosmological studies (Zhang 2008). These effects can degrade the evidence of accelerating expansion, or even mimic the dark energy behavior. So comprehensive study of the cosmic opacity is needed. Especially for the Wide Field Infrared Survey Telescope (WFIRST) era, which can detect more than 2000 SNe Ia (Green et al. 2012). If the cosmic opacity is not corrected, it will not increase statistical errors, but may also systematically bias the cosmological parameters.

Over the past several years, the cosmic distance duality (CDD) relation has been widely used to test the systematic errors and opacity in SNe Ia observations. The CDD relation reads (Etherington 1933; Ellis 2007)

$$\frac{D_L}{D_A}(1+z)^{-2} = 1, \quad (1)$$

where D_L is the luminosity distance, and D_A is the angular diameter distance. We must note that the cosmic opacity has no effect on the angular diameter D_A (Weinberg 2008). It is valid for all cosmological models based on Riemannian geometry. The bases of this relation are that the number of photons is conservative and the photons travel along the null geodesics in a Riemannian spacetime (Ellis 2007). But the conservation of photons may be violated in a wide range of well-motivated models. In modern astronomy, the CDD relation plays a significant role. In order to test this relation, many works have been performed. For example, Bassett & Kunz (2004) found a 2σ violation of CDD relation using D_L from SNe Ia and D_A from FRIIb radio galaxies. The angular diameter from X-ray observations of galaxy clusters also has been used to probe the CDD relation (Holanda et al. 2011). Similar works have also been done by other authors (Meng et al. 2012; Goncalves et al. 2012). Räsänen et al. (2016) used CMB anisotropies to test the CDD relation. This relation is also applied extensively. Wang et al. (2012) and Cao et al. (2016) used the CDD relation to test the gas mass density profile of galaxy clusters. Evslin (2016) calibrated the distances of SNe Ia using the CDD relation.

A powerful method to study the opacity of the universe is using the standard candles to

detect possible CDD deviations, such as SNe Ia and GRBs. For example, Avgoustidis et al. (2010) adopted a modified CDD relation

$$D_L = D_A(1+z)^{2+\varepsilon} \quad (2)$$

to constrain the cosmic opacity by combining the SNe Ia data (Kowalski et al. 2008) with the measurements of the Hubble expansion over redshift range $0 < z < 2$ (Stern et al. 2010). In the flat Λ CDM model, they found $\varepsilon = -0.04^{+0.08}_{-0.07}$ (2σ). In Avgoustidis et al. (2009), they marginalized over the parameter H_0 and used SNe Ia alone to constrain parameters Ω_m and ε . Li et al. (2013) presented some tests for the cosmic opacity with observational data including the Union 2.1 SNe Ia sample and galaxy cluster samples compiled by Filippis et al. (2005) and Bonamente et al. (2006). They found that an almost transparent universe is favored by the sample (Li et al. 2013). Basing on the validity of the Amati relation, Holanda et al. (2014) determined the cosmic opacity at high redshifts using GRBs, and found that a transparent universe is favored. Strong gravitational lensing systems are also used to probe the CDD relation (Liao et al. 2015; Holanda et al. 2016).

Compared with previous papers, our paper has three advancements to this field. First, it must be noted that previous studies directly used the luminosity distances of SNe Ia, which are derived in the concordance cosmology (i.e., Avgoustidis et al. 2010; Li et al. 2013). The luminosity distances depend on the light-curve fitting parameters and cosmological models (Kowalski et al. 2008; Betoule et al. 2014). So the derived results are biased by the assumed cosmological model. Here, in order to avoid this problem, we perform a global fitting for the SNe Ia light-curve parameters, cosmological parameters and cosmic opacity. Second, we also investigate the cosmic opacity at high redshifts, where the fraction of electrons is evolving with redshift. The reionization process is considered. The cross section of Compton scattering for high-energy photons is also a function of redshift. Third, the contribution from Compton scattering effect to the cosmic opacity is constrained for the first time. In this paper, we investigate the cosmic opacity with SNe Ia, long GRBs and Hubble parameter data. We pay special attention to the Compton scattering effect. This paper is organized as follows. In next section, we describe the cosmic opacity and Compton scatter extinction. In section 3, the observational data used in the statistical analysis are presented. The corresponding constraints on the cosmic opacity are given in section 4. The paper is finished with a summary of the main results in the conclusion section.

2. Cosmic opacity and Compton scattering

Since photons can be scattered with free electrons and interstellar medium when travel from the source to the observer, the received photons number will be reduced. The distance

modulus derived from standard candles will increase the systematic error. Any process reducing photon number would increase the luminosity distance of the source and dim its luminosity. Following Avgoustidis et al. (2009), we regard $\tau(z)$ as the opacity from the $z = 0$ to the resource redshift due to extinction. Then, the received flux will decrease with a factor $e^{-\tau(z)}$. So the relation between observed luminosity distance $D_{L,obs}$ and theoretic luminosity distance $D_{L,th}$ is

$$D_{L,obs} = D_{L,th} e^{\frac{\tau(z)}{2}}. \quad (3)$$

The observed distance modulus is given by

$$\mu_{obs}(z) = \mu_{th}(z) + 2.5(\log_{10}(e))\tau(z). \quad (4)$$

For flat FLRW cosmology, the distance modulus is

$$D_{L,th}(z) = (1+z) \frac{c}{H_0} \int_0^z \frac{dz}{E(z)}, \quad (5)$$

and

$$E(z) = H(z)/H_0 = \sqrt{\Omega_m(1+z)^3 + (1-\Omega_m)(1+z)^{3+3w}}. \quad (6)$$

Combining equations (2) and (3), we obtain the exactly form of cosmic opacity

$$\tau = 2\varepsilon \ln(1+z). \quad (7)$$

2.1. The optical depth of Compton scattering

Compton scattering is the inelastic scattering of the photon by a charged free electron. The optical depth for Compton scattering is

$$\tau_c(z) = \int \sigma_T n_e(z) dl = -(1+y)\sigma_T c \int_0^z n_H(z) Q_{HII}(z) \frac{dt}{dz} dz, \quad (8)$$

where σ_T is the Thomson cross section, n_e is the free electron density, c is the light speed, and z is the redshift. In the above equation, $n_H(z) = 1.905 \times 10^{-7}(1+z)^3 \text{ cm}^{-3}$ is the hydrogen number density at redshift z , and y is a factor which is introduced by including the ionization of helium. Because the reionization epoch contains both hydrogen and helium. The mass fractions of hydrogen and helium are $X = 1 - Y$ and $Y = 0.24668$ (Planck Collaboration 2016), respectively. We assume that the helium was only ionized once. So we derive $y = Y/(4X) \approx 0.082$. $Q_{HII}(z)$ is defined as the volume filling fraction of ionized hydrogen, which can be calculated from the differential equation (Madau et al. 1999; Barkana & Loeb 2001; Wang 2013)

$$\dot{Q}_{HII} = \frac{\dot{n}_\gamma(z)}{(1+y)n_H(z)} - \alpha_B C(z)(1+y)n_H(z)Q_{HII}. \quad (9)$$

In this equation, $\alpha_B = 2.6 \times 10^{-13} \text{ cm}^{-3}\text{s}^{-1}$ is the recombination coefficient for electron with temperature at about 10^4 K . $\dot{n}_\gamma(z)$ is the rate of ionizing photons escaping from the stars into the IGM, which can be derived from

$$\dot{n}_\gamma(z) = (1+z)^3 \frac{\dot{\rho}_*(z)}{m_B} N_\gamma f_{esc}, \quad (10)$$

where $(1+z)^3$ is used for converting the comoving density into the proper density, $\dot{\rho}_*(z)$ is the star formation rate (SFR), m_B is the baryon mass, N_γ are the number of ionizing UV photons released per baryon, and f_{esc} is the escape fraction of these photons from stars into IGM. The escape fraction is not well constrained from observations. $f_{esc} \leq 0.2$ is the average value suggested by Mao et al. (2007) and Robertson et al. (2015). Other similar value are reported. For instance, Razoumov & Sommer-Larsen (2006) found that f_{esc} evolves from $\sim 1 - 2$ percent at $z = 2.39$ to $\sim 6 - 10$ percent at $z = 3.6$ from star forming regions in young galaxies. Hayes et al. (2011) proposed a redshift evolution of f_{esc} . In this work, we take the value of N_γ as ~ 4000 and the escape fraction $f_{esc} \simeq 0.1$. $C \equiv \langle n_{HII}^2 \rangle / \langle n_{HII} \rangle^2$ is the clumping factor of the ionized gas. Its value decreases with increasing redshifts from some numerical simulations (Gnedin & Ostriker 1997; Shull et al. 2012) and semi-analytical studies (Madau et al. 1999; Chiu & Ostriker 2000). Following Shull et al. (2012), we take

$$C(z) = \begin{cases} 2.9 & \text{if } z < 5, \\ 2.9(\frac{1+z}{6})^{-1.1}, & \text{if } z \geq 5. \end{cases} \quad (11)$$

$\dot{\rho}_*(z)$ is the SFR. The SFR derived by Wang (2013) is used. Then we can solve the differential equation (9) to obtain Q_{HII} . The result is shown in figure 1.

2.2. The Compton scattering optical depth for SNe Ia

Following Hu (1995) and Barkana & Loeb (2001), the equation (8) with a constant ionization fraction can be expressed as

$$\tau_c(z) = 0.0461(1+y)Q_{HII}(1-Y_p)\frac{\Omega_b h}{\Omega_m}\{[1 - \Omega_m + \Omega_m(1+z)^3]^{\frac{1}{2}} - 1\}, \quad (12)$$

in the flat Λ CDM model by neglecting the radiation term. At redshift range $0 < z < 3$, a constant ionization fraction $X_e(z) = 1$ is adopted, which is reasonable for SNe Ia. The optical depth can increase the distance modulus with a relation $\Delta\mu = 1.086\tau$ from equation (4). Figure 2 shows the Compton scattering effect on the distance modulus. From this figure, we can see that the value of $\Delta\mu$ is increasing with redshift, and the Compton scattering dims the supernova flux by 0.003 mag at $z = 1$ and 0.01 mag at $z = 2.35$, respectively. This

dimming is too faint to rule out the existence of dark energy. However, its effect can not be negligible for future SNe Ia surveys plan such as WFIRST, which will measure ~ 2700 SNe Ia to $z \sim 1.7$. For future surveys, the major statistical uncertainty is the SN intrinsic fluctuations. With the SNe Ia number N , the intrinsic fluctuations are reduced to a level of σ_μ/\sqrt{N} mag, where σ_μ is the intrinsic dispersion in SN luminosity. It means that the Compton dimming effect must be corrected. Otherwise the induced systematic errors would be comparable to the statistical errors. From above analysis, we conclude that the Compton scattering can be correctable, as discussed by Zhang (2008).

2.3. The Compton scattering dimming for GRBs

The photons emitted from GRBs are different from those from SNe Ia. First, the energy of the GRB photons are much more energetic. At high energies, cross section of the Compton scattering is suppressed. So more photons can escape from scattering to the observer. Second, GRBs can be observed at high redshifts. High-energy photons have much more probability to interact with free electrons. The optical depth of Compton scattering for high-energy photons can be written as

$$\tau_c(z) = -(1+y)c \int_0^z \sigma(x)n_H(z)Q_{HII}(z)\frac{dt}{dz}dz, \quad (13)$$

where $\sigma(x) = \sigma(E_0(1+z)/m_e c^2)$ is given by the Klein-Nishina formula (Rybicki & Lightman 1976)

$$\sigma(x) = \frac{3}{4}\sigma_T[(1+x)\frac{2x(1+x)/(1+x) - \ln(1+2x)}{x^3} + \frac{\ln(1+2x)}{2x} - \frac{1+3x}{(1+2x)^2}]. \quad (14)$$

Here, E_0 is the observed energy of γ -ray photons. The future SOVM (Space-based multi-band astronomical Variable Objects Monitor) mission, will detect some GRBs at $z > 10$ (Wei et al. 2016). At these high-redshifts, the hydrogen is not completely ionized. The parameter Q_{HII} is a constant in equation (13), and the reionization process must be considered. We use the reionization process described in Section 2.1 to calculate the optical depth. The systematic shift in distance modulus $\Delta\mu$ due to Compton scattering is shown in figure 3. It is obvious that the effect of Compton scattering for low-energy photons is significant, because the cross section is suppressed for high-energy photons. The evolution of $\Delta\mu$ becomes flat at high redshifts, due to few free electrons from reionization. The $\Delta\mu$ caused by Compton dimming increases with redshift. Its value can reach to 0.01-0.04 mag, which is smaller than the intrinsic error of GRB distance (Wang et al. 2016). So we can ignore it if the number of GRBs is less than 100 and the redshift of GRB is not very high.

However, if more than 100 high-redshift long GRBs will be used to study cosmology, the Compton dimming is non-negligible.

3. Data set

In this section, we will show the data sets. These data sets will be used to constrain the cosmic opacity and cosmological parameters. Unlike previous works, we try to global fit the SNe Ia light-curve parameters, cosmological parameters and the cosmic opacity.

3.1. SNe Ia sample

In this work, we use 740 SNe Ia from the “joint light-curve analysis” sample compiled by Betoule et al. (2014). The redshift range is from 0.01 to 1.299. This sample includes SNe Ia from different surveys. In their work, they regard the possible extinction as systematic uncertainty. In order to avoid the effect of cosmological model effect, the parameters of the SNe Ia light-curve, cosmological parameters and the cosmic opacity are fitting simultaneously. Therefore, only the statistical error which from error propagation of light-curve fitting uncertainties and the variation of magnitudes caused by the intrinsic variation in SN magnitude are needed to consider in our work. The possible extinctions are all regarded as cosmic opacity. The distance modulus is written as

$$\mu = m_B^* - (M_B - \alpha \times X_1 + \beta \times C), \quad (15)$$

where m_B^* is the observed peak magnitude in rest-frame B band. α and β are nuisance parameters which describe the stretch-luminosity and color-luminosity relations, reflecting the well-known broader-brighter and bluer-brighter relations, respectively. The nuisance parameter M_B represents the absolute magnitude of a fiducial SNe Ia and is found to depend on the properties of host galaxies, e.g., the host stellar mass (M_{stellar}). Here, we follow the procedure in Conley et al. (2011) to approximately correct for this effect by a simple step function:

$$M_B = \begin{cases} M_B^1 & \text{if } M_{\text{stellar}} < 10^{10} M_{\odot}, \\ M_B^1 + \Delta_M & \text{otherwise.} \end{cases} \quad (16)$$

3.2. GRB sample

For GRBs, we use the GRB data given in Wang et al. (2016). They use the $E_{\text{iso}}-E_p$ correlation Amati et al. (2002) to build the Hubble diagram. Wang et al. (2016) combine

their 42 GRBs and 109 GRBs from Amati et al. (2008) and Amati et al. (2009). The E_{iso} - E_p correlation can be written as

$$\log \frac{E_{iso}}{\text{erg}} = c + d \log \frac{E_p}{\text{keV}}, \quad (17)$$

where parameters c and d are free parameters, E_{iso} is the isotropic equivalent energy, and E_p is the peak energy of νF_ν spectrum, which has been corrected into the cosmological rest frame. In their work, they calibrate 90 high-redshift GRBs in the redshift range from 1.44 to 8.1 with a fixed value of H_0 . We constrain the cosmological parameters and the cosmic opacity use this sub-sample (Wang et al. 2016). In order to consider the effect of Compton dimming, we show the value of $\Delta\mu$ for this sample as dots in figure 3, which is derived from equations (4) and (13). The error bar is due to the uncertainty of the observational peak energy of GRBs. The value of $\Delta\mu$ caused by Compton dimming is far less than the top black dash line. Therefore, we can ignore this effect in following work.

3.3. $H(z)$ sample

The 19 Hubble parameter data given in Simon et al. (2005), Stern et al. (2010), and Moresco et al. (2012) are used in this work. The redshift range of these Hubble parameters is from 0.10 to 1.75. Because H_0 will affect the final results, we regard H_0 as a free parameter.

4. Results

The maximum likelihood analysis is used to constrain the parameters. The χ^2 fitting expression is

$$\chi^2 = \sum_i^n \frac{[\mu_{obs} - \mu_{th}(z_i) - 1.086\tau(z_i)]^2}{\sigma_\mu^2} + \chi_{H(z)}^2 \quad (18)$$

In our analysis, we adopt the cosmic opacity from equation (7). The parameter ε is regarded as a constant. For data of SNe Ia and $H(z)$, The μ_{obs} for SNe Ia is written as equation (15). $\sigma_\mu^2 = \sigma_{\mu,stat}^2 + \sigma_{\mu,sys}^2$ is the distance modulus uncertainty. $\sigma_{\mu,stat}^2$ is the propagated error from the covariance matrix of the light-curve fitting, and $\sigma_{\mu,sys}$ is the systematic error due to the intrinsic variation in SNe Ia magnitude. The value $\sigma_{\mu,sys}$ is calculated in Betoule et al. (2014), which is not depend on a specific choice of cosmological model. μ_{th} is the theoretic distance modulus which is depend on cosmological model. $\chi_{H(z)}^2$ is the χ^2 fitting of Hubble parameter data, which can be calculated by

$$\chi_{H(z)}^2 = \sum_i^m \frac{[H_{obs}(z_i) - H_{th}(z_i)]^2}{\sigma_{H_{obs}}^2}, \quad (19)$$

where the H_{obs} is the observation value, H_{th} is the theoretic Hubble expansion rate related to cosmological model, and $\sigma_{H_{obs}}$ is the error of H_{obs} . For the GRB data, because Wang et al. (2016) calibrated the distance moduli by fixing $H_0 = 67.8 \text{ km s}^{-1} \text{ Mpc}^{-1}$, so the value of H_0 is fixed when using the GRB data. We use the Markov chain Monte Carlo (MCMC) method to fit the parameters of the SNe Ia light-curve, cosmological parameters and the cosmic opacity simultaneously. Our program is based on the public emcee Python module (Foreman-Mackey et al. 2013). The algorithm of emcee has several advantages over traditional MCMC methods and it has excellent performance as measured by the autocorrelation time.

4.1. Flat Λ CDM

In this model, the equation of state w in equation (6) has a fixed value with $w = -1$. When using the SNe Ia + $H(z)$ data, the free parameters are M_B , α , β , ΔM , H_0 , Ω_m , and ε . We use the emcee Python module to fit these parameters simultaneously. The fitting result is shown in figure 4. The 2-D regions and 1-D marginalized distributions with 1σ and 2σ contours for the parameters M_B , α , β , ΔM , H_0 , Ω_m , and ε are shown. The fitting results of parameters are presented in table I. The value of ε is $0.0226^{+0.0403}_{-0.0451}$, which indicates an almost transparent universe. For GRB+ $H(z)$ data, there are only two free parameters: Ω_m and ε . The fitting results are shown in figure 5 and table I. The value $\varepsilon = 0.00718^{+0.0486}_{-0.0492}$ also supports a transparent universe.

4.2. Flat XCDM

In a flat XCDM cosmology, the parameter w in equation(6) is a free parameter. When using the SNe Ia + $H(z)$ data, the free parameters are M_B , α , β , ΔM , H_0 , Ω_m , w and ε . Using the same method as above, we can perform the simultaneously fitting of these parameters. The 2-D regions and 1-D marginalized distributions with 1σ and 2σ contours for the parameters M_B , α , β , ΔM , H_0 , Ω_m , and ε are shown in figure 6 and table I. They are shown in the fourth and the last column of table I. The value of ε is $0.0517^{+0.0617}_{-0.0659}$. For GRB+ $H(z)$ data, there are three parameters: Ω_m , w and ε . The fitting results are shown in figure 7 and table I. The value $\varepsilon = 0.0718^{+0.0497}_{-0.0491}$ also indicates a transparent universe.

4.3. Considering the effect of Compton dimming

Because the effect of Compton dimming can be estimated, the residual opacity can be derived. We try to eliminate the known opacity due to Compton scattering, and explore the contribution by unknown part. In the equation (12), we get the optical depth of Compton scattering of SNe Ia. After subtracting the optical depth of Compton scattering from total cosmic opacity, we repeat the above analysis to obtain the residual opacity τ_r . In flat Λ CDM model, the results from SNe Ia + $H(z)$ are shown in figure 8, which gives $\varepsilon = 0.0212^{+0.0382}_{-0.0413}$. Constraints on parameters are shown in the column 3 of table I. Similar results are also shown in figure 8 and column 5 of table I for XCDM model. Comparing the second and third columns in table I, it can be seen that the effect of Compton scattering can cause about 5% cosmic opacity in Λ CDM model. For XCDM model, a similar percentage is found. So Compton scattering can contribute about a few percent of cosmic opacity. It's obvious that the sample supports an almost transparent universe for both cosmological models.

5. Conclusions and discussion

In this paper, we use the latest observations, including SNe Ia from JLA sample and Hubble parameters, to study cosmic opacity. The effect of Compton scattering on standard candles is also considered. The extinction due to Compton scattering can be correctable in future SNe Ia survey. In order to avoid the cosmological dependence of SNe Ia luminosity distances, a joint fitting of the SNe Ia light-curve parameters, cosmological parameters and opacity is used. In order to explore the cosmic opacity at high redshifts, the latest gamma-ray bursts (GRBs) are used. Because some instruments will detect high-redshift GRBs in future, the reionization process must be considered for Compton scattering. The result shows that the Compton dimming effect is less than the systematic error for GRBs at present. However, if more than 100 high-redshift long GRBs are observed and used to constrain cosmological parameters, the Compton dimming is non-negligible. The results support an almost transparent universe at $z < 1.5$ for JLA SNe Ia and $H(z)$ data. In the redshift range $1.5 < z < 8.1$, we study the cosmic opacity through luminosity distances of GRBs. The flat Λ CDM model and the flat XCDM model are considered. We find that the effect of Compton scattering can cause about 5% cosmic opacity in both models. The current observations support an almost transparent universe for both cosmological models at a large redshift range.

Acknowledgements

We thank the anonymous referee for useful comments. This work is supported by the National Basic Research Program of China (973 Program, grant No. 2014CB845800), the National Natural Science Foundation of China (grants 11422325 and 11373022), and the Excellent Youth Foundation of Jiangsu Province (BK20140016).

REFERENCES

- Amati, L., Frontera, F., Tavani, M., et al., 2002, A&A, 390, 81
- Amati, L., Guidorzi, C., Frontera, F., et al. 2008, MNRAS, 391, 577
- Amati L., Frontera, F., & Guidorzi, C., 2009, A&A, 508, 173
- Avgoustidis, A., Burrage, C., Redondo, J., Verde, L. & Jimenez, R., 2009, JCAP, 06, 012.
- Avgoustidis, A., Burrage, C., Redondo, J., Verde, L. & Jimenez, R., 2009, JCAP, 10, 024
- Barkana, R., & Loeb, A. 2001, PhR, 349, 125
- Betoule, M., et al., 2014, A&A, 568, A22
- Bassett, B., A., & Kunz, M., 2004, PRD, 69, 101305
- Cao, S., et al., 2016, MNRAS, 457, 281
- Capozziello, S., 2002, Int. J. Mod. Phys. D, 11, 483
- Chiu, W. A. & Ostriker, J. P. 2000, ApJ, 534, 507
- Combes, F., 2004, New Astronomy Rev, 48, 583
- Conley, A., et al., 2011, ApJS, 192, 1
- Drell, P. S., Loredo, T. J., & Wasserman, I., 2000, ApJ, 530, 593
- Eisenstein, D. J., et al. 2005, ApJ, 633, 560
- Ellis, G. F. R., 2007, Gen. Relativ. Gravit , 39, 1047
- Etherington, I. M. H., 1933, Philos. Mag, 15, 761
- Evslin, J., 2016, PDU, 14, 57

- Foreman-Mackey, D., Hogg, D.W., Lang, D., Goodman, J., 2013, PASP, 125, 306
- Gnedin, N. Y., & Ostriker, J.P., 1997, ApJ. 486, 581
- Goncalves, R. S., Holanda, R. F. L., & Alcaniz, J. S., 2012, MNRAS, 420, L43
- Green, J., et al., 2012, arXiv: 1208.4012
- Filippis, E. De., Sereno, M., Bautz W., & Longo, G., 2005, ApJ, 625, 108
- Hayes, M., Schaerer, D., Östlin, G., et al. 2011, ApJ, 730, 8
- Holanda, R. F. L., Lima, J. A. S., & Ribeiro, M. B., 2011, A&A, 528 , L14
- Holanda, R. F. L. & Busti, V. C., 2014, Phys. Rev. D, 89, 103517
- Holanda, R. F. L. & Busti, V. C., 2016, JCAP, 89, 103517
- Holz, D. E. 1998, ApJ, 506, L1
- Hu, W., 1995. Ph.D. Thesis, astro-ph/9508126
- Hui, L. & Greene, P., 2006, PRD, 73, 123526
- Jimenez, R., Verde, L., Treu, T., Stern, D., 2003, ApJ, 593, 622
- Kowalski et al. 2008, ApJ, 686, 749
- Li, Z. X., Wu, P. X., Yu, H. W., & Zhu, Z. H., 2013, PRD, 87, 103013
- Liao, K., Li, Z. X., Cao, S., Biesiada, M., Zheng, X. G., & Zhu, Z. H., 2015, ApJ, 822, 2
- Bonamente, M., Joy, M. K., LaRoque, S. J., Carlstrom, J.E., Reese, E. D., & Dawson, K. S., 2006, ApJ, 647, 25.
- Madau, P., Haardt, F., & Rees, M. J. 1999, ApJ, 514, 648
- Mao, J., Lapi, A., Granato, G. L., de Zotti, G., & Danese, L. 2007, ApJ, 667, 655
- Meng, X. L., Zhang, T. J., Zhan, Hu., & Wang, Xin., 2012, ApJ, 745, 98
- Moresco, M. et al., 2012, JCAP, 08, 006
- Perlmutter, S., et al. 1999, ApJ, 517, 565
- Planck Collaboration, Ade, P. A. R., et al., 2016, A&A, 594, A13

- Räsänen, S., Valiviita, J. & Kosonen, V., 2016, JCAP, 04, 050
- Razoumov, A. O., & Sommer-Larsen, J., 2006, ApJ, 651, L89
- Riess, A. G., et al. 1998, AJ, 116, 1009
- Rybicki, G.B. & Lightman, A.P., 1979, *Radiative Processes in Astrophysics*. John Wiley & Sons, Inc.
- Robertson, B. E., Ellis, R. S., Furlanetto, S. R., & Dunlop, J. S., 2015, ApJL, 802, L19
- Shull J. M., Harness A., Trenti M. & Smith B. D., 2012, ApJ, 747, 100
- Simon, J., Verde, L., & Jimenez, R., 2005, PRD, 71, 123001
- Spergel, D. N., et al. 2003, ApJS, 148, 175
- Stern, D., Jimenez, R., Verde, L., Stanford, S. A., & Kamionkowski, M., 2010, ApJS, 188, 280
- Tan, W. W., Wang, F. Y., & Cheng, K. S., 2016, ApJ, 829, 29
- Wang, F. Y., 2013, A&A, 556, A90
- Wang, F. Y., Dai, Z. G. & Liang, E. W., 2015, New Astro. Rev., 67, 1
- Wang, J. S., Wang, F. Y., Cheng, K. S., & Dai, Z. G., 2016, A&A, 13, 9
- Wang, X., Meng, X. L., Huang, Y. F., & Zhang, T. J., 2012, A&A, 585, A68
- Wei, J., et al., 2016, arXiv:1610.06892, SVOM white book
- Weinberg, S., 2008, *Cosmology*, Oxford University Press
- Zhang, P. J., 2008, ApJ, 682, 721

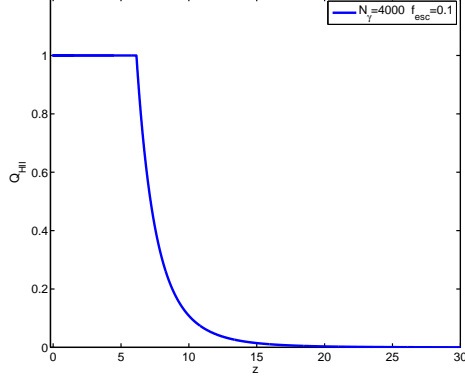


Fig. 1.— H_{II} filling factor $Q_{H_{II}}$ as a function of redshift calculated for the $f_{esc} = 0.1$ and $N_\gamma = 4000$.

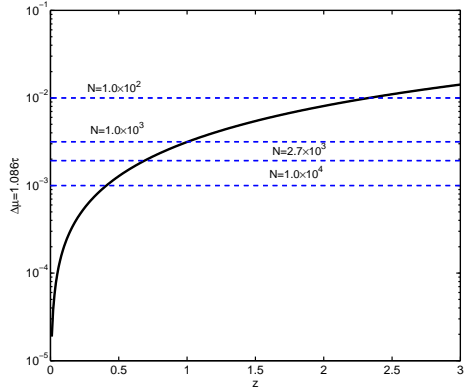


Fig. 2.— Systematic shift in the distance modulus μ caused by Compton scattering (solid line). The dimming is 0.3% in flux at $z = 1$ and 1% at $z = 2.35$ with Compton dimming effect. The statistical errors for 100, 1000, 2700 and 10000 SNe are shown as the dash lines. We adopt intrinsic dispersion $\sigma_\mu = 0.1$ mag for SNe Ia.

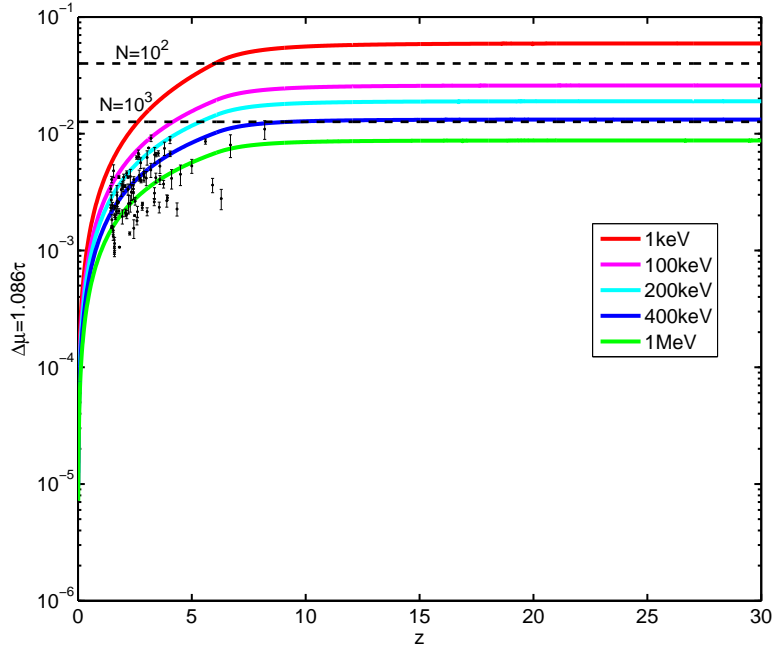


Fig. 3.— The systematic shift in distance moduli $\Delta\mu$ for GRBs. We consider the ionization fraction as a function of redshift. The Compton scattering cross section is energy dependent, because the photons of GRBs are energetic. The statistical errors for 100 and 1000 GRBs are shown by the dash lines, respectively. We adopt intrinsic dispersion $\sigma_\mu = 0.4$ mag for GRBs. The black dots are the $\Delta\mu$ of observed GRBs caused by Compton dimming.

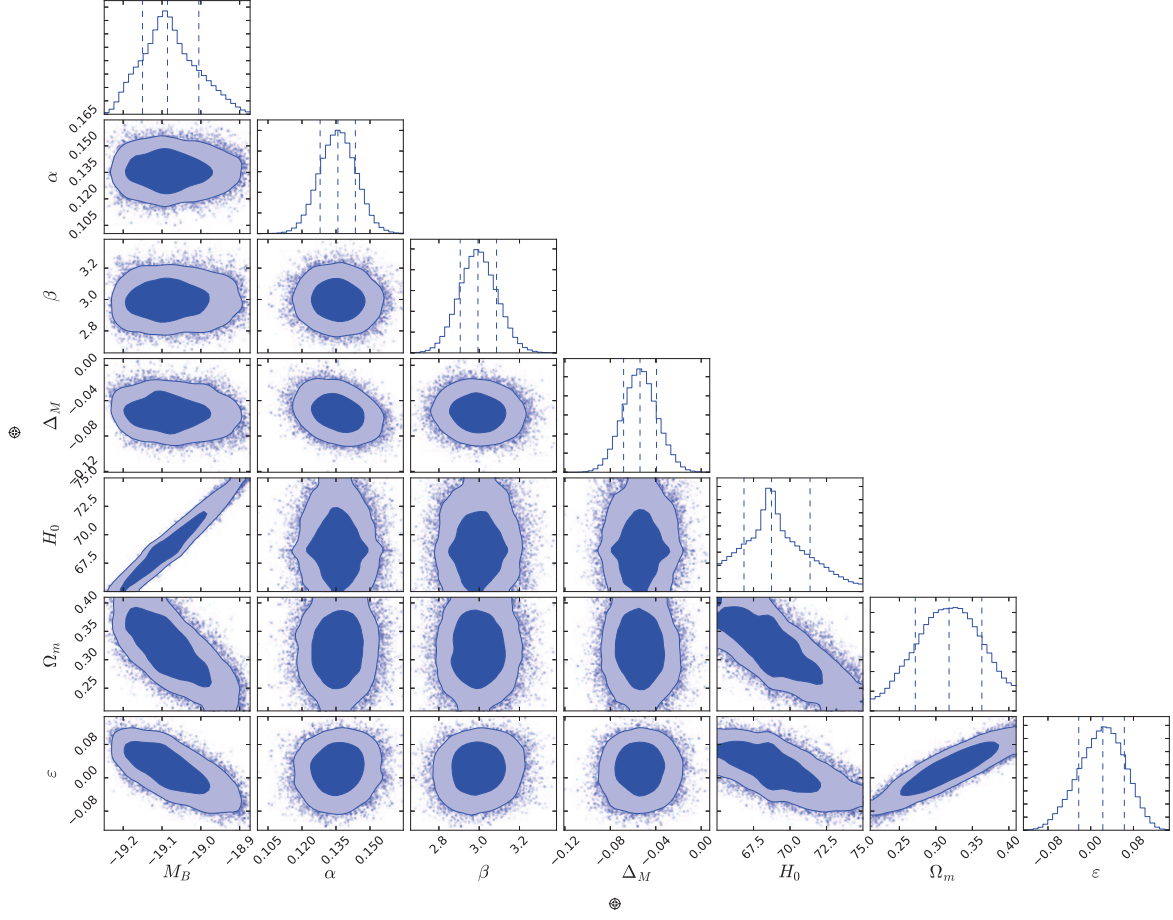


Fig. 4.— In Λ CDM model, the 2-D regions and 1-D marginalized distributions with 1σ and 2σ contours for the parameters M_B , α , β , Δ_M , H_0 , Ω_m , and ε using SNe Ia+ $H(z)$.

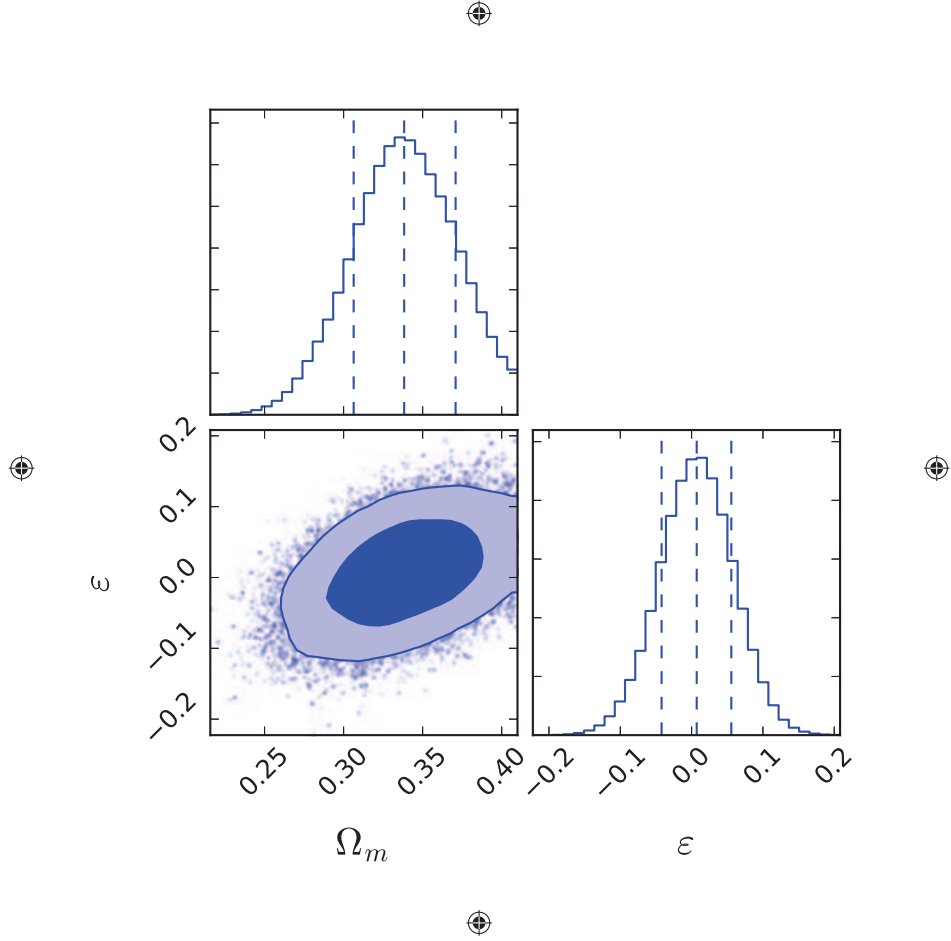


Fig. 5.— The 2 - D regions and 1 - D marginalized distributions with 1σ and 2σ contours for the parameters Ω_m , ϵ using GRBs+ $H(z)$ in Λ CDM model.

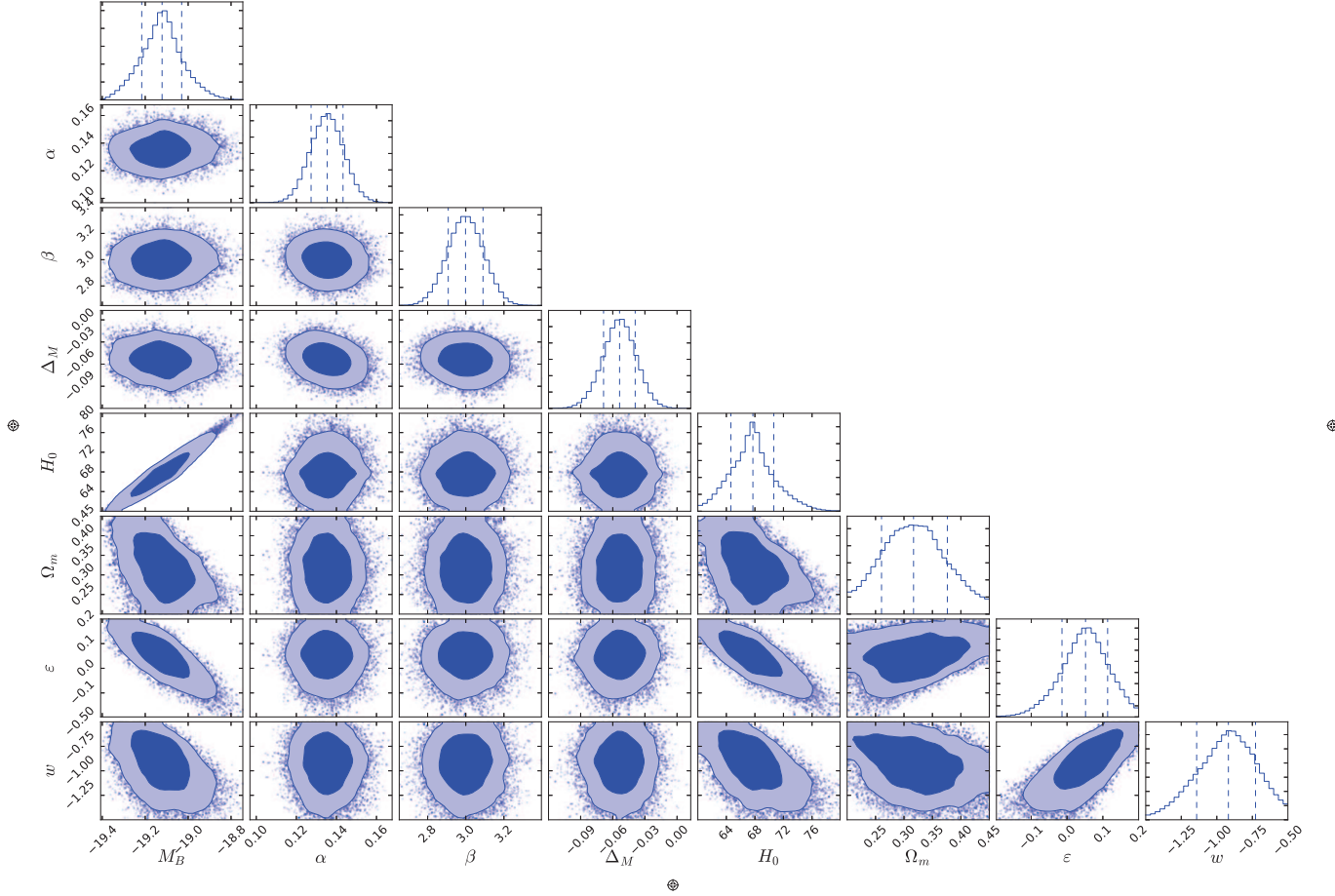


Fig. 6.— In XCDM model, 2 - D regions and 1 - D marginalized distributions with 1σ and 2σ contours for the parameters M_B , α , β , Δ_M , H_0 , Ω_m , ε using SNe Ia+ $H(z)$.

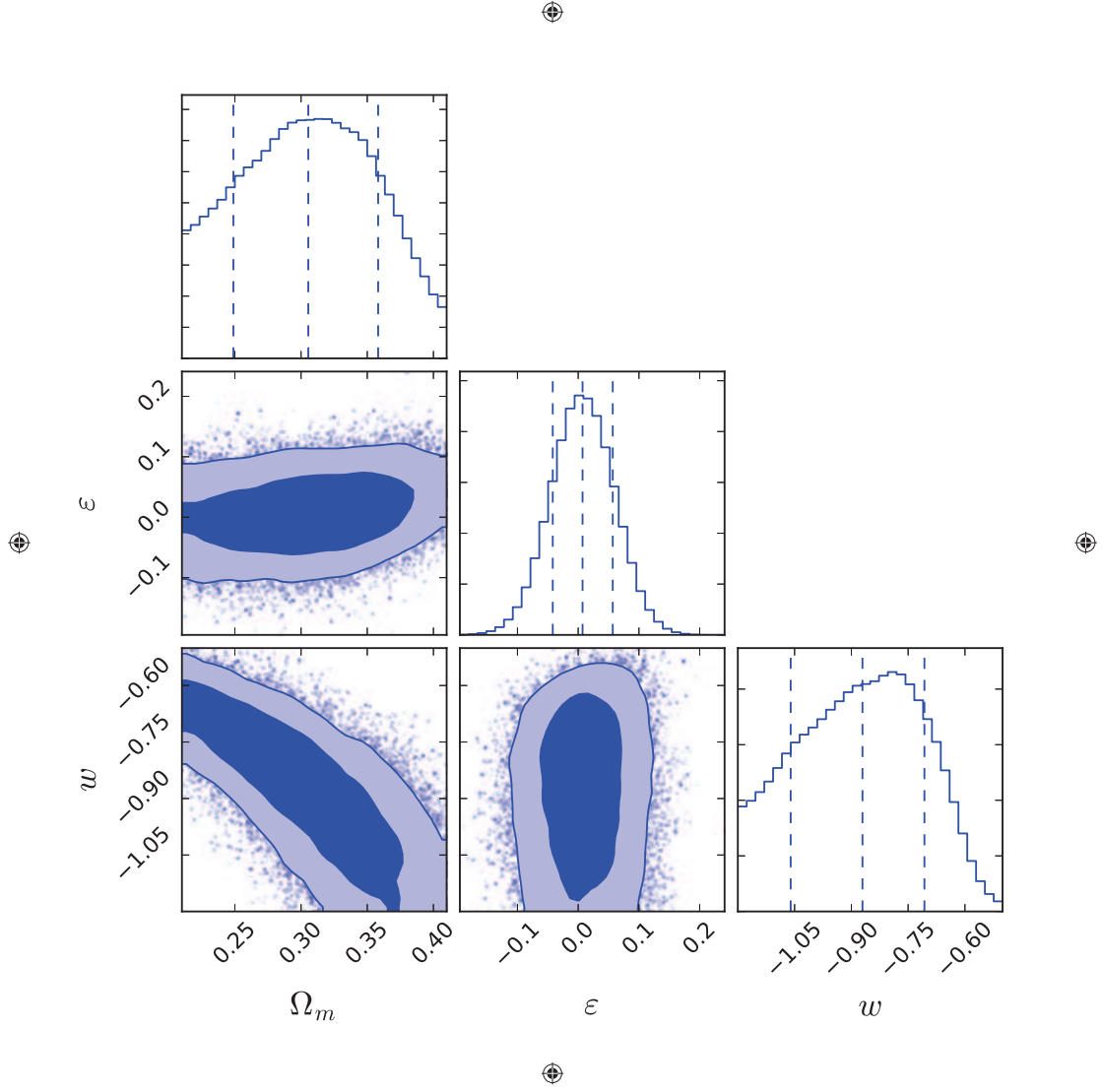


Fig. 7.— In XCDM model, 2 - D regions and 1 - D marginalized distributions with 1σ and 2σ contours for the parameters Ω_m , ε using GRBs+ $H(z)$.

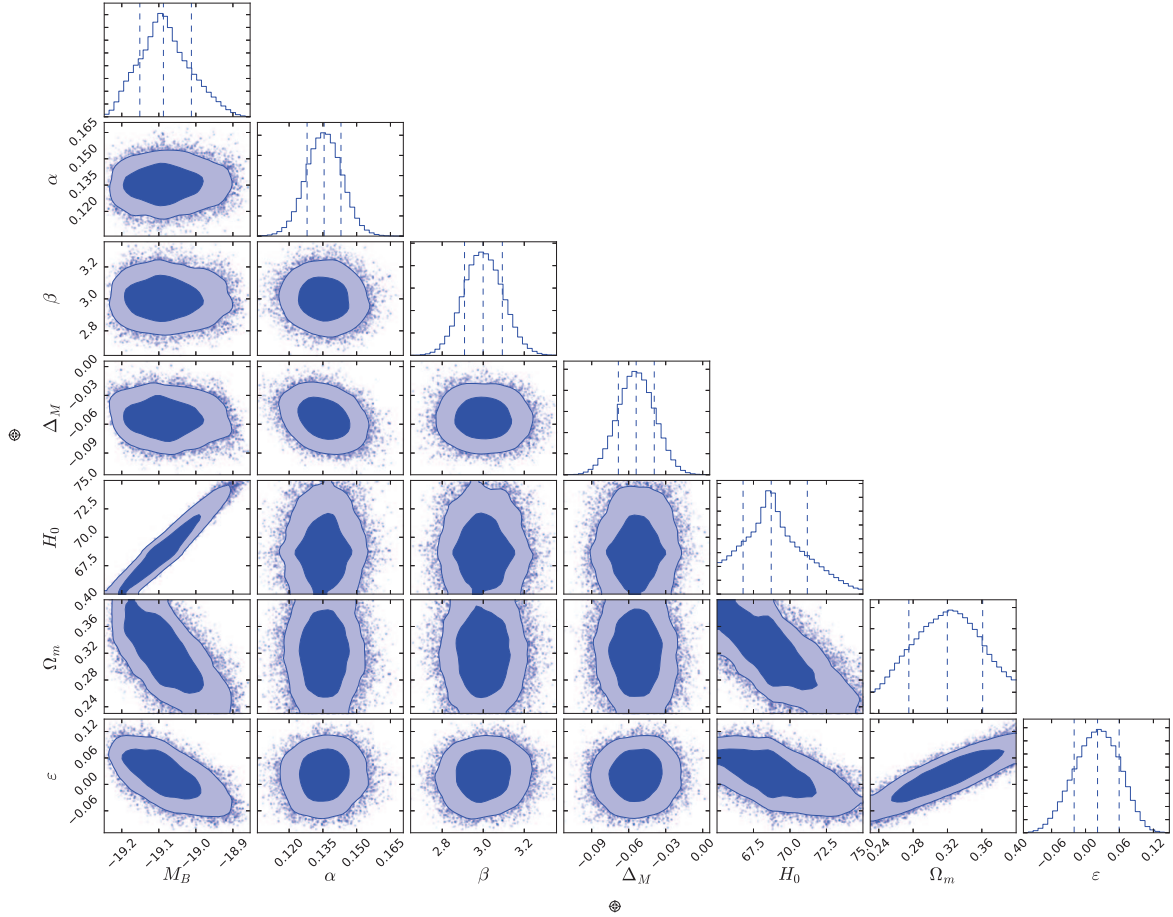


Fig. 8.— In Λ CDM model, 2 - D regions and 1 - D marginalized distributions with 1σ and 2σ contours for the parameters M_B , α , β , Δ_M , H_0 , Ω_m , and ε using SNe Ia+ $H(z)$ after subtracting the effect of Compton scattering.

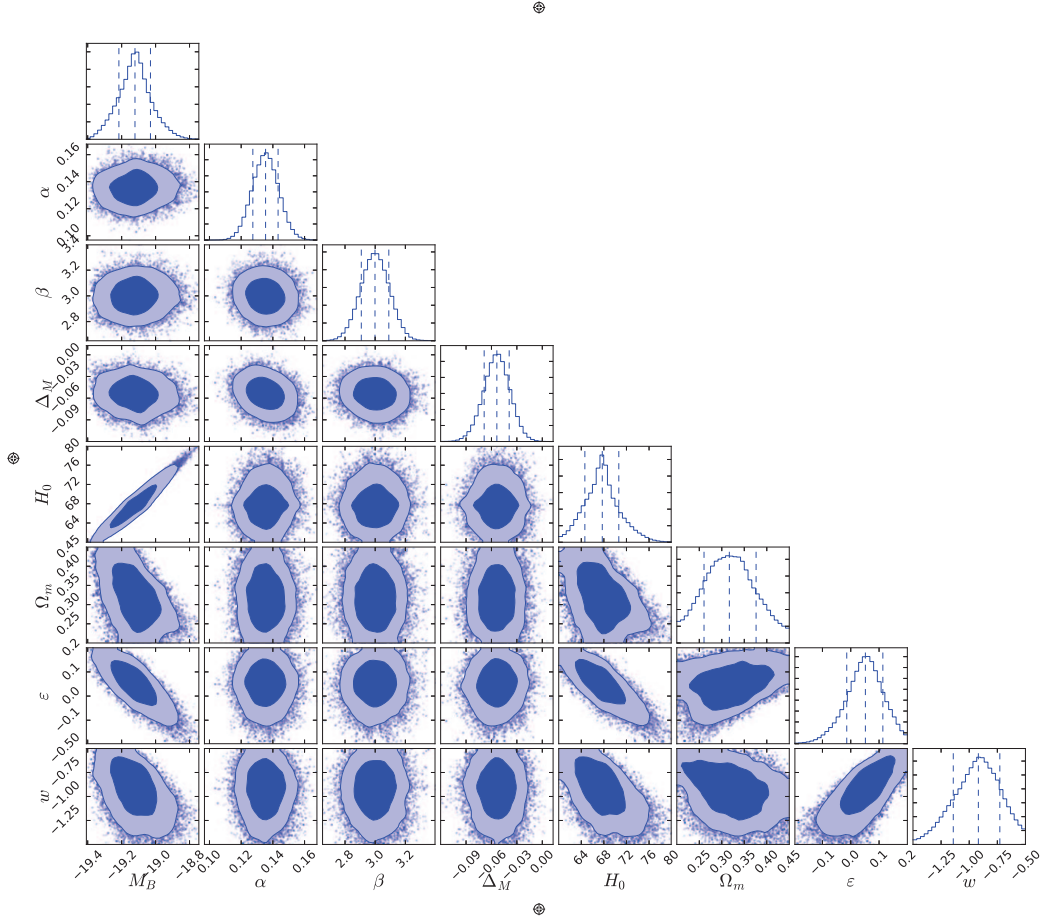


Fig. 9.— In XCDM model, 2 - D regions and 1 - D marginalized distributions with 1σ and 2σ contours for the parameters M_B , α , β , Δ_M , H_0 , Ω_m , and ε using SNe Ia+ $H(z)$ after subtracting the effect of Compton scattering.

Table 1: Constraints on ε , light-curve parameters and cosmological parameters with 1σ confidence level in different models.

| Model | Λ CDM | | | XCDM | | |
|---------------|-------------------------------|-------------------------------|-------------------------------|-------------------------------|-------------------------------|------------------------------|
| data set | H(z)+SNe Ia | | H(z)+GRBs | H(z)+SNe Ia | | H(z)+GRBs |
| $\tau(z)$ | $2\varepsilon \ln(1+z)$ | subtracting τ_c | $2\varepsilon \ln(1+z)$ | $2\varepsilon \ln(1+z)$ | 2subtracting τ_c | $2\varepsilon \ln(1+z)$ |
| a | $0.136^{+0.00772}_{-0.00783}$ | $0.136^{+0.00749}_{-0.00756}$ | / | $0.135^{+0.00790}_{-0.00803}$ | $0.136^{+0.00780}_{-0.00773}$ | / |
| b | $2.994^{+0.0923}_{-0.0878}$ | $3.000^{+0.0937}_{-0.0908}$ | / | $2.999^{+0.0916}_{-0.0907}$ | $3.002^{+0.0896}_{-0.0893}$ | / |
| M_B | $-19.086^{+0.0807}_{-0.0643}$ | $-19.088^{+0.0756}_{-0.0638}$ | / | $-19.121^{+0.0913}_{-0.0948}$ | $-19.113^{+0.0868}_{-0.0854}$ | / |
| Δ_M | $-0.0539^{+0.0145}_{-0.0145}$ | $-0.0539^{+0.0147}_{-0.0144}$ | / | $-0.0536^{+0.0146}_{-0.0150}$ | $-0.0543^{+0.0142}_{-0.0152}$ | / |
| H_0 | $68.732^{+2.641}_{-1.884}$ | $68.715^{+2.474}_{-1.929}$ | 67.8 fixed | $67.718^{+2.923}_{-3.085}$ | $67.857^{+2.917}_{-2.738}$ | 67.8 fixed |
| Ω_m | $0.318^{+0.0449}_{-0.0462}$ | $0.320^{+0.0412}_{-0.0448}$ | $0.338^{+0.0325}_{-0.0319}$ | $0.317^{+0.0594}_{-0.0563}$ | $0.308^{+0.0536}_{-0.0553}$ | $0.305^{+0.0528}_{-0.0569}$ |
| w | / | / | / | $-0.919^{+0.191}_{-0.223}$ | $-0.906^{+0.200}_{-0.205}$ | $-0.871^{+0.164}_{-0.190}$ |
| ε | $0.0226^{+0.0403}_{-0.0451}$ | $0.0212^{+0.0382}_{-0.0413}$ | $0.00718^{+0.0486}_{-0.0492}$ | $0.0517^{+0.0617}_{-0.0659}$ | $0.0490^{+0.0590}_{-0.0654}$ | $0.0718^{+0.0497}_{-0.0491}$ |